Commun. Theor. Phys. (Beijing, China) **37** (2002) pp 465–474

Vol. 37, No. 4, April 15, 2002

Calculation of Double-Differential Cross Sections of n+^{7}Li Reactions Below 20 MeV

ZHANG Jing-Shang and HAN Ying-Lu

China Institute of Atomic Energy, P.O. Box 275(41), Beijing 102413, China

(Received July 22, 2001)

Abstract *A new reaction model for light nuclei is proposed to analyze the measured data, especially for analysis of the double-differential cross sections of the outgoing particles. Many channels are opened in the $n + {}^7Li$ reaction below $E_n < 20$ MeV. The reaction mechanism is very complex, beside the sequential emissions there are also three-body breakup processes. Because of a strong recoil effect of light nucleus reactions, the energy balance is strictly taken into account. The comparisons of the calculated results with the double-differential measurements indicate that the model calculations are successful for the total outgoing neutrons.*

PACS numbers: 25.10.+s
Key words: light nucleus reactions, double-differential cross sections, discrete levels

1 Introduction

With the abundance 92.5% of ^{7}Li in lithium element, the neutron interaction with ^{7}Li is important from the application point of view, accompanying with the evaluated data of ^{6}Li needed in thermonuclear fusion reactor system. On the other hand the reaction mechanism of $n + {}^7$Li is very complex, there are many opened reaction channels below 20 MeV. Besides the sequential particle emissions, the cluster separation and three-body breakup process like $^6\mathrm{He} \to n + n + \alpha$ are also involved. The total neutron energy-angular spectra consist of the outgoing neutrons from various reaction channels, which strongly differ from each other. The double differential cross sections could provide the information for analyzing the components from the differential reaction mechanism. A new method has been proposed for neutron induced reactions on light nuclei, and analyzed the energy-angular spectra of n+^{12}C,[1] n+^{6}Li[2] and n+^{16}O[3] successfully. Now this approach has been applied for $n + {}^7$Li reaction. The neutron energy-angular spectra have been measured by Baba at E_n = 5.1, 6.6, and 15.4 MeV in 1979.[4] Afterwards, Chiba and Xia measured the neutron energy-angular spectra at E_n = 14.2 MeV in 1985[5] and in 1993,[6] respectively. Recently Chiba measured neutron energy-angular spectra at E_n = 11.5 and 18 MeV.[7] These double measurements provide the analytic data based for this work.

In view of the emission processes for $n + {}^7$Li reactions below 20 MeV, all of the emissions proceed from the compound nucleus of ^{8}Li to the discrete levels of the residual nuclei. This kind of reactions can be described based on the unified Hauser–Feshbach and exciton model.[8]

The phenomenological spherical optical potential is used in the model calculations. The neutron optical model parameters are determined by fitting the total, elastic scattering, non-elastic cross sections and elastic-scattering angular distributions. The optical model parameters of charged particles like protons, deuterons, and tritons are determined by fitting the corresponding reaction cross sections.

Since the pre-equilibrium emission is the important reaction mechanism from the compound nucleus to the discrete levels of the residual nuclei, each of which has its individual spin and parity, the angular momentum coupling effect must be taken into account for angular momentum conservation.[3] Three motion systems are used in this model calculation, the physical quantity is indicated by the superscripts l, c, and r for the laboratory system (LS), the center of mass system (CMS) and the recoil residual nucleus system (RNS), respectively.

In Sec. 2 the reaction channels of $n + {}^7$Li are listed in detail. The representations of double-differential cross sections of sequential particle emissions for cluster separation have been obtained,[1] which are used for the second emitted particles in the $(n, 2n)$, (n, np), (n, nd), (n, nt), and (n, pn) reaction channels of $n + {}^7$Li. The energy-angular spectra of the second particle emissions from discrete level to discrete level have a ring-type form in CMS. This type of double-differential cross sections is called D to D for short. Meanwhile, equations (19) $\sim$ (29) in Ref. [1] are used for the cluster separation of ^{5}He as the residual nucleus of the reaction channel (n, nd). ^{5}He is unstable and separated spontaneously into a neutron and an alpha particle with Q = 0.894 MeV, each cluster has definite value of outgoing energy in RNS. Since the cluster separation comes from a ring-type spectrum, which is treated as a continuum spectrum, so this type of double-differential cross sections is called C to D for short. Since all of the formulae mentioned above have been given in Ref. [1], so in this paper we do not repeat the representations. In the case of n+^{7}Li reactions there are three-body breakup processes from the excited state of ^{6}He as the residual nucleus of the reaction channels (n, np), (n, pn),

as well as $(n,\ d)$. The ground state of ^{6}He only has the β^- decay. The first excited state of ^{6}He has the energy of $E_{k=1}(^6\mathrm{He}) = 1.797$ MeV, while the neutron binding energy is 1.869 MeV, so it could not emit the neutron, only decays via three-body breakup into two neutrons and an alpha particle with the Q value of $Q_3 = -0.973$ MeV. The formula of three-body breakup processes from the discrete levels of the residual nucleus of $(n,\ d)$ channel is given in Ref. [2], which is called D to C for short. But in the case of $n + ^7$Li reactions the three-body breakup from $(n,\ np)$, $(n,\ pn)$ channels are the emission processes from continuum spectra to continuum states, which is called C to C for short. This kind of description for the three-body breakup process is presented in detail in Sec. 3.

Because of the level widths and energy resolution in the measurements, according to the Heisenberg's uncertainty relation, the measured data are always in a broadening form. Therefore, in fitting procedure the broadening effect must be taken into account with the Gaussian expansion form. Since all of the calculations are carried out in CMS, so that the transformation from CMS to LS must be performed in the fitting procedure. The formulation of the broadening expansions and the formulation of the motion system transformation can be found in the Sec. 5 of Ref. [1].

The calculated energy-angular distributions of outgoing neutrons at $E_n = 5.1$, 6.6, 11.5, 14.2, and 18 MeV are shown in Figs 1 $\sim$ 10 in Sec. 4. Because of the very low excited energy 0.478 MeV of the first excited level of ^{7}Li, so that the inelastic scattering spectrum is overlapped by the elastic scattering peak. This situation is shown in Fig. 11. The calculated results of the outgoing neutrons agree fairly well with the experimental data. The analysis of the contribution from the individual components at $E_n = 11.5$ is shown in Fig. 12. A summary is given in Sec. 5.

2 The Reaction Channels of $n + ^7$Li Reaction

The reaction channels of $n + ^7$Li reactions for $E_n \leqslant 20$ MeV are listed as follows:

$$n + {}^7\mathrm{Li} = \begin{cases} \gamma + {}^8\mathrm{Li}, & Q = 2.033\ \mathrm{MeV}, \\ n' + {}^7\mathrm{Li}^*, & Q = -0.4776\ \mathrm{MeV}, \\ d + {}^6\mathrm{He}, & Q = -7.750\ \mathrm{MeV}, \\ t + {}^5\mathrm{He}, & Q = -3.3362\ \mathrm{MeV}, \\ 2n + {}^6\mathrm{Li}, & Q = -7.249\ \mathrm{MeV}, \\ n, p + {}^6\mathrm{He}, & Q = -9.974\ \mathrm{MeV}, \\ n, d + {}^5\mathrm{He}, & Q = -9.618\ \mathrm{MeV}, \\ n, t + \alpha, & Q = -2.467\ \mathrm{MeV}, \\ 2n, p + {}^5\mathrm{He}, & Q = -11.842\ \mathrm{MeV}, \\ 2n, d + \alpha, & Q = -8.724\ \mathrm{MeV}, \end{cases}$$

The discrete level schemes of every reaction channel at $E_n \leqslant 20$ MeV are taken from Ref. [9]. The reaction situation from the compound nucleus ^{8}Li* to the discrete levels of the residual nuclei up to 20 MeV is presented in Tables 1 and 2, respectively. One can see that the first excited level of ^{7}Li cannot emit any particle, so it purely contributes to the inelastic-scattering channel. The second and the third excited level of ^{7}Li can only emit triton, so they purely contribute to the $(n, nt\alpha)$ reaction channel. Above the fourth excited level of ^{7}Li the second neutron emissions appear, while the levels above the seventh excited level can emit proton. In this case the emission branching ratios can be obtained by means of the model calculation to issue the competition.

Table 1 The reaction situation from the compound nucleus ^{8}Li* to the discrete levels of the residual nuclei from $(n,\ n')$, $(n,\ d)$, $(n,\ t)$, and $(n,\ 2n)$ reactions up to 20 MeV.

	E_{th}[a]	k_1	k_2	$(p+R)_3$[b]	Channel
$(n,n')\,^7$Li	0.5463	1			(n,n')
$(n,d)\,^6\mathrm{He}_{g,s}$	8.868	gs[c]			(n,d)
$(n,d)\,^6$He*	9.978	1			$(n,2nd)\alpha$
$(n,t)\,^5$He	3.845	gs $-$ 2			$(n,na)t$
$(n,2n)\,^6$Li	8.532	4	gs	$Y + {}^6$Li	$(n,2n)\,^6$Li
$(n,2n)\,^6$Li	11.06	5	gs, 2	$Y + {}^6$Li	$(n,2n)\,^6$Li
$(n,2n)\,^6$Li	11.06	5	1	$d + \alpha$	$(n,2nd)\alpha$
$(n,2n)\,^6$Li	11.266	6	gs, 2	$Y + {}^6$Li	$(n,2n)\,^6$Li
$(n,2n)\,^6$Li	11.266	6	1	$d + \alpha$	$(n,2nd)\alpha$
$(n,2n)\,^6$Li	12.856	7	gs, 2	$Y + {}^6$Li	$(n,2n)\,^6$Li
$(n,2n)\,^6$Li	12.856	7	1, 3	$d + \alpha$	$(n,2nd)\alpha$
$(n,2n)\,^6$Li	15.670	8	gs, 2	$Y + {}^6$Li	$(n,2n)\,^6$Li
$(n,2n)\,^6$Li	15.670	8	1, 3 $-$ 5	$d + \alpha$	$(n,2nd)\alpha$
$(n,2n)\,^6$Li	15.670	8	4 $-$ 5	$p + {}^5$He	$(n,3np)\alpha$
$(n,2n)\,^6$Li	16.813	9	gs, 2	$Y + {}^6$Li	$(n,2n)\,^6$Li
$(n,2n)\,^6$Li	16.813	9	1, 3 $-$ 5	$d + \alpha$	$(n,2nd)\alpha$
$(n,2n)\,^6$Li	16.813	9	4 $-$ 5	$p + {}^5$He	$(n,3np)\alpha$

[a] The term E_{th} refers to the threshold energy needed to open the k_2 level of the residual nucleus via the k_1 level in unit of MeV (As the same as in Table 2).

[b] The acronym $(p+R)_3$ refers to the third emitted particle and its residual nucleus.

[c] The acronym gs stands for the ground state (As the same as in Table 2).

It must be stressed that all of the excited levels of ^{6}Li can emit the secondary particle like neutron, proton and deuteron, except the second excited level (3.563 (0^+)),[2]

which only decays by gamma emission, so the $(n, 2n)$ reaction channel comes from the two neutron emissions reaching to the ground state and the second excited state of ^{6}Li. The (n, d) reaction channel comes from the deuteron emission to the ground state of ^{6}He with the threshold energy of 8.868 MeV, while the deuteron emission to the first excited state of ^{6}He* contributes to the $(n, 2nd)\alpha$ channel via three-body breakup process ($^6\mathrm{He} \to n + n + \alpha$) with the threshold energy of 9.978 MeV. Meanwhile the reaction channels $(n, pn)^6$He* and $(n, 2np)^5$He belong to $(n, 3np)\alpha$ channel. From Table 1 one can see that the fourth and the fifth excited levels of ^{6}Li can emit proton with the residual nucleus ^{5}He to open $(n, 3np)$ reaction channel, which needs the eighth excited level of ^{7}Li* to be reached from the compound nucleus ^{8}Li* by the first neutron emission with the threshold energy of 15.670 MeV.

Table 2 The reaction situation from the compound nucleus ^{8}Li* to the discrete levels of the residual nuclei of the (n, np), (n, nd), and (n, pn) reaction channels up to 20 MeV.

	E_{th}	k_1	k_2	Channel
$(n,np)\,^6\mathrm{He}_g$	12.856	7	gs	(n,np)
$(n,np)\,^6\mathrm{He}_g$	15.670	8	gs	(n,np)
$(n,np)\,^6\mathrm{He}^*$	15.670	8	1	$(n,2nd)\alpha$
$(n,np)\,^6\mathrm{He}$	16.813	9	gs	(n,np)
$(n,np)\,^6\mathrm{He}^*$	16.813	9	1	$(n,2nd)\alpha$
$(n,nd)\,^5\mathrm{He}$	11.060	5	gs	$(n,2nd)\alpha$
$(n,nd)\,^5\mathrm{He}$	11.266	6	gs	$(n,2nd)\alpha$
$(n,nd)\,^5\mathrm{He}$	12.856	7	gs	$(n,2nd)\alpha$
$(n,nd)\,^5\mathrm{He}$	15.670	8	gs − 1	$(n,2nd)\alpha$
$(n,nd)\,^5\mathrm{He}$	16.813	9	gs − 1	$(n,2nd)\alpha$
$(n,nt)\alpha$	5.296	2	gs	$(n,nt)\alpha$
$(n,nt)\alpha$	7.64	3	gs	$(n,nt)\alpha$
$(n,nt)\alpha$	8.532	4	gs	$(n,nt)\alpha$
$(n,nt)\alpha$	11.06	5	gs	$(n,nt)\alpha$
$(n,nt)\alpha$	11.266	6	gs	$(n,nt)\alpha$
$(n,nt)\alpha$	12.856	7	gs	$(n,nt)\alpha$
$(n,nt)\alpha$	15.670	8	gs	$(n,nt)\alpha$
$(n,nt)\alpha$	16.813	9	gs	$(n,nt)\alpha$
$(n,pn)\,^6\mathrm{He}_g$	11.919	9	gs	$(n,np)\,^6\mathrm{He}_g$

3 Three-Body Breakup Process

The kinetics of the three-body breakup process has been given by Ohlsin.[10] The analytical expression of the double-differential cross section is obtained by

$$\frac{\mathrm{d}^2\sigma}{\mathrm{d}\epsilon_i\,\mathrm{d}\Omega_i} = \frac{\sigma}{4\pi}S(\epsilon_i), \qquad i = 1,2,3\,, \tag{1}$$

here the normalized spectrum satisfies $\int_{\epsilon_{1(\min)}}^{\epsilon_{1(\max)}} S(\epsilon_i)\,\mathrm{d}\epsilon_i = 1$ and the explicit expression reads

$$S(\epsilon_i) = \frac{8}{\pi\epsilon_{i(\max)}^2}\sqrt{\epsilon_i(\epsilon_{i(\max)} - \epsilon_i)}\,, \tag{2}$$

where $\varepsilon_{i(\max)}$ is the maximum outgoing energy of the ith particle and $E_{\mathrm{brk}} = E_{k=1}(^6\mathrm{He}) - Q_3 = 0.824$ MeV stands for the energy released from the first excited state of ^{6}He in the three-body breakup process. So the final state of the three-body breakup process is a continuum spectrum with $\varepsilon_{i(\min)} = 0$ and

$$\epsilon_{i(\max)} = \frac{M - m_i}{M}E_{\mathrm{brk}}, \qquad i = 1,2,3\,, \tag{3}$$

where M is the mass of ^{6}He, m_i refers to the mass of the ith outgoing particle in three-body breakup process. The energy carried by each particle is obtained by

$$E_i = \int_0^{\epsilon_{i(\max)}} \epsilon_i S(\epsilon_i)\,\mathrm{d}\epsilon_i = \frac{1}{2}\epsilon_{i(\max)}\,, \quad i = 1,2,3\,. \tag{4}$$

It is easy to prove that the total energy carried by the three particles is obtained by $E_1 + E_2 + E_3 = E_{\mathrm{brk}}$. Thus the energy balance is held analytically.

When ^{6}He* is yielded as the residual nucleus of the reaction channel ^{7}Li$(n, np+pn)$ in the case of three-body breakup process, the particle is emitted from a ring-type spectrum of the residual nucleus to continuum spectrum, so the reaction description is from a continuum state to a continuum state (C to C for short). We denote m_2 and M_2 as the masses of the second emitted particle and its residual nucleus. B_2 refers to the binding energy of the emitted second particle. Therefore, the normalized double-differential cross section of the ith particle is given by

$$\frac{\mathrm{d}^2\sigma}{\mathrm{d}\epsilon_i^c\,\mathrm{d}\Omega_i^c} = \int \mathrm{d}E_{M_2}^c\,\mathrm{d}\Omega_{M_2}^c \frac{\mathrm{d}^2\sigma}{\mathrm{d}E_{M_2}^c\,\mathrm{d}\Omega_{M_2}^c}\sqrt{\frac{\epsilon_i^c}{\epsilon_i^r}}\frac{S(\epsilon_i^r)}{4\pi} \equiv \sum_l \frac{2l+1}{4\pi}f_l(\epsilon_i^c)\mathrm{P}_l(\cos\theta_i^c)\,. \tag{5}$$

The normalized double-differential cross section of the residual nucleus M_2 is given by using the Legendre expansion form as

$$\frac{\mathrm{d}^2\sigma}{\mathrm{d}E_{M_2}^c\,\mathrm{d}\Omega_{M_2}^c} = \sum_l \frac{2l+1}{4\pi}f_l(E_{M_2}^c)\mathrm{P}_l(\cos\theta_{M_2}^c)\,. \tag{6}$$

Multiplying $\mathrm{P}_l(\cos\theta_i^c)$ on both sides of Eq. (5), and integrated over Ω_i^c the Legendre coefficient of the ith particle

in CMS is obtained by

$$f_l(\epsilon_i^c) = \frac{1}{4\pi}\int \frac{\mathrm{d}^2\sigma}{\mathrm{d}E^c_{M_2}\,\mathrm{d}\Omega^c_{M_2}}\sqrt{\frac{\epsilon_i^c}{\epsilon_i^r}} \times S(\epsilon_i^r)\mathrm{P}_l(\cos\theta_i^c)\,\mathrm{d}E^c_{M_2}\,\mathrm{d}\Omega^c_{M_2}\,\mathrm{d}\Omega^c_i\,. \quad (7)$$

If Θ is the angle between $\vec{\Omega}^c_{M_2}$ and $\vec{\Omega}^r_i$, by using the relation in Eq. (6),

$$\mathrm{P}_L(\cos\theta^c_{M_2}) = \frac{4\pi}{2L+1}\sum_m \mathrm{Y}^*_{Lm}(\Theta,\Phi)\mathrm{Y}_{Lm}(\Omega^c_i)\,. \quad (8)$$

Carrying out the integration over $\cos\Theta$ and Φ, then the Legendre coefficient becomes into the form

$$f_l(\epsilon_i^c) = \frac{1}{2}\int f_l(E^c_{M_2})\sqrt{\frac{\epsilon_i^c}{\epsilon_i^r}}S(\epsilon_i^r)\mathrm{P}_l(\cos\Theta)\,\mathrm{d}E^c_{M_2}\,\mathrm{d}\cos\Theta\,. \quad (9)$$

Changing integration variable from $\cos\Theta$ to ϵ_i^r, equation (9) becomes into the following form

$$f_l(\epsilon_i^c) = \frac{1}{4}\sqrt{\frac{M_2}{m_i}}\int_A^B \mathrm{d}E^c_{M_2}\frac{f_l(E^c_{M_2})}{\sqrt{E^c_{M_2}}}\int_a^b \frac{\mathrm{d}\epsilon_i^r}{\sqrt{\epsilon_i^r}}S(\epsilon_i^r)\mathrm{P}_l\left(\frac{\epsilon_i^c+\dfrac{m_i}{M_2}E^c_{M_2}-\epsilon_i^r}{2\sqrt{\dfrac{m_i}{M_i}E^c_{M_2}\epsilon_i^c}}\right)\,. \quad (10)$$

For the given values of ϵ_i^c and $E^c_{M_2}$, by using the composition of velocities but written in energy scale, the integration limits of ϵ_i^r are obtained by

$$a = \left(\sqrt{\epsilon_i^c} - \sqrt{\frac{m_i}{M_2}E^c_{M_2}}\right)^2, \qquad b = \min\left\{\epsilon^r_{i(\max)}, \left(\sqrt{\epsilon_i^c} + \sqrt{\frac{m_i}{M_2}E^c_{M_2}}\right)^2\right\}. \quad (11)$$

The integration limits A and B of $E^c_{M_2}$ for a given ϵ_i^c are given by

$$A = \begin{cases} \dfrac{M_2}{m_i}\left(\sqrt{\epsilon_i^c} - \sqrt{\epsilon^r_{i(\max)}}\right)^2, & \text{if} \quad \sqrt{\epsilon^r_{i(\max)}} + \sqrt{\dfrac{m_i}{M_2}E^c_{M_2,\min}} \le \sqrt{\epsilon_i^c}\,, \\ E^c_{M_2,\min}, & \text{otherwise}\,, \end{cases} \quad (12)$$

$$B = \min\left\{E^c_{M_2,\max}, \frac{M_2}{m_i}\left(\sqrt{\epsilon_i^c} + \sqrt{\epsilon^r_{i(\max)}}\right)^2\right\}. \quad (13)$$

The energy region of the ring-type spectrum of the residual nucleus M_2 is given by (see Sec. 3 of Ref. [1])

$$E^c_{M_2,\min} = E_2^r(1-\gamma_{M_2})^2, \qquad E^c_{M_2,\max} = E_2^r(1+\gamma_{M_2})^2\,, \quad (14)$$

$$\gamma_{M_2} = \sqrt{\frac{E^c(M_1)M_2}{E_2^r M_1}}, \qquad E_2^r = \frac{m_2}{M_1}(E_{k_1} - B_2 - E_k)\,. \quad (15)$$

The energy region of the ith particle from the three-body breakup process in CMS is given by

$$\epsilon^c_{i(\max)} = \left(\sqrt{\frac{m_i}{M_2}}E^c_{M_2,\max} + \sqrt{\epsilon^r_{i(\max)}}\right)^2, \quad (16)$$

$$\epsilon^c_{i(\min)} = \begin{cases} \left(\sqrt{\dfrac{m_i}{M_2}E^c_{M_2,\min}} - \sqrt{\epsilon^r_{i(\max)}}\right)^2, & \text{if} \quad \epsilon^r_{i,(\max)} < \dfrac{m_i}{M_2}E^c_{M_2,\min}\,, \\ 0, & \text{otherwise}\,. \end{cases} \quad (17)$$

In the case of C to C, the spectrum of $f_0(\epsilon_i^c)$ is normalized. In fact, by exchanging the order of the integration variable one get

$$\int_{\epsilon^c_{i(\min)}}^{\epsilon^c_{i(\max)}} f_0(\epsilon_i^c)\,\mathrm{d}\epsilon_i^c = \frac{1}{4}\sqrt{\frac{M_2}{m_i}}\int_{E^c_{M_2,\min}}^{E^c_{M_2,\max}}\mathrm{d}E^c_{M_2}\frac{f_0(E^c_{M_2})}{\sqrt{E^c_{M_2}}}\int_0^{\epsilon^r_{i(\max)}}\frac{\mathrm{d}\epsilon_i^r}{\sqrt{\epsilon_i^r}}S(\epsilon_i^r)\int_{\left(\sqrt{m_i E^c_{M_2}/M_2}-\sqrt{\epsilon_i^r}\right)^2}^{\left(\sqrt{m_i E^c_{M_2}/M_2}+\sqrt{\epsilon_i^r}\right)^2}\mathrm{d}\epsilon_i^c$$

$$= \frac{1}{4}\sqrt{\frac{M_2}{m_i}}\int_{E^c_{M_2(\min)}}^{E^c_{M_2(\max)}}\mathrm{d}E^c_{M_2}\frac{f_0(E^c_{M_2})}{\sqrt{E^c_{M_2}}}\int_0^{\epsilon^r_{i(\max)}}\frac{\mathrm{d}\epsilon^r_{m_i}}{\sqrt{\epsilon^r_{m_i}}}S(\epsilon^r_{m_i})4\sqrt{\frac{m_i}{M_2}E^c_{M_2}\epsilon_i^r}$$

$$= \int_{E^c_{M_2(\min)}}^{E^c_{M_2(\max)}} \mathrm{d}E^c_{M_2} f_0(E^c_{M_2}) = 1\,. \tag{18}$$

The representation of $f_0(E^c_{M_2})$ is given in Ref. [1] as

$$f_0(E^c_{M_2}) = \frac{1}{4\gamma_{M_2} E^r_2}\,. \tag{19}$$

The first excited level of ^{6}He from $(n,\ np+pn)$ channel decays by three-body breakup process into two neutrons and an alpha particle, all of them belong to $(n,\ 3np)\alpha$ reaction channel.

The energy carried by the ith particle from the three-body breakup process in CMS can be calculated by

$$\begin{aligned} E^c(m_i) &= \int_{\epsilon^c_{i(\min)}}^{\epsilon^c_{i(\max)}} \epsilon^c_i f_0(\epsilon^c_i)\,\mathrm{d}\epsilon^c_i \\ &= \frac{1}{4}\sqrt{\frac{M_2}{m_i}} \int_{E^c_{M_2,\min}}^{E^c_{M_2,\max}} \mathrm{d}E^c_{M_2} \frac{f_0(E^c_{M_2})}{\sqrt{E^c_{M_2}}} \int_0^{\epsilon^r_{i(\max)}} \frac{\mathrm{d}\epsilon^r_i}{\sqrt{\epsilon^r_i}} S(\epsilon^r_i) \int_{\left(\sqrt{m_i E^c_{M_2}/M_2}-\sqrt{\epsilon^r_i}\right)^2}^{\left(\sqrt{m_i E^c_{M_2}/M_2}+\sqrt{\epsilon^r_i}\right)^2} \epsilon^c_i\,\mathrm{d}\epsilon^c_i \\ &= \frac{m_i}{M_2} \int_{E^c_{M_2,\min}}^{E^c_{M_2,\max}} E^c_{M_2} f_0(E^c_{M_2})\mathrm{d}E^c_{M_2} + \int_0^{\epsilon^r_{i(\max)}} S(\epsilon^r_i)\epsilon^r_i\,\mathrm{d}\epsilon^r_i \\ &= \frac{m_i}{M_2}E^r_2 + \frac{m_i}{M_1}E^c(M_1) + \frac{1}{2}\epsilon^r_{i(\max)}\,. \end{aligned} \tag{20}$$

The explicit expressions of E^r_2 and $E^c(M_1)$ can be found in Ref. [1] (see Eqs (4) and (44)). The energy carried by the second emitted particle in CMS is (see Eq. (48) of Ref. [1])

$$E^c(m_2) = \frac{M_2}{M_1}(E_{k_1} - B_2 - E_{k_2}) + \frac{m_2}{M_1}\frac{m_1}{M_C}(E^* - B_1 - E_{k_1})\,. \tag{21}$$

In LS the energy carried by m_2 is (see Eq. (50) of Ref. [1])

$$E^l(m_2) = \frac{m_n m_2}{M_C^2}E_n + E^c(m_2) - 2\frac{m_2}{M_C}\sqrt{\frac{m_n}{M_1}E_n E^c(M_1)}\; f^c_1(m_1)\,. \tag{22}$$

The energy carried by the first emitted particle m_1 in LS is given by (see Eq. (45) of Ref. [1])

$$E^l(m_1) = \frac{m_n m_1}{M_C^2}E_n + \frac{M_1}{M_C}(E^* - B_1 - E_{k_1}) + 2\frac{M_1}{M_C}\sqrt{\frac{m_n}{M_1}E_n E^c(M_1)}\; f^c_1(m_1)\,. \tag{23}$$

The energy carried by the ith particle from the three-body breakup process in LS is

$$E^l(m_i) = \frac{m_n m_i}{M_c^2}E_n + E^c(m_i) - 2\frac{m_i}{M_c}\sqrt{\frac{m_n}{M_1}E_n E^c(M_1)}\; f^c_1(m_1)\,. \tag{24}$$

Therefore, the total released energy is obtained by

$$\begin{aligned} E^l_T &= E^l(m_1) + E^l(m_2) + \sum_{i=1,2,3} E^l(m_i) \\ &= E_n + B_n - B_1 - B_2 - Q_3 = E_n + Q\,, \end{aligned} \tag{25}$$

where $Q = -10.948$ MeV is the Q-value of the reaction channel $(n,\ 3np)\alpha$. Thus the energy balance is still held exactly in the C to C reaction mechanism.

4 Results and Discussions

The LUNF code for $n + ^7$Li is developed for calculating the reaction cross sections and the energy-angular spectra of all kinds of outgoing particles from $n+^7$Li reactions below 20 MeV. The comparisons of the calculated results with the double-differential measurement are shown in Fig. 1 at an incident neutron energy $E_n = 5.1$ MeV for outgoing angles of 30°, 45°, 60°, 75°, 90°, and 120°, respectively. The comparisons of that are shown in Figs 2 and 3 at an incident neutron energy $E_n = 6.6$ MeV for outgoing angles of 30°, 45°, 60°, 75°, 90°, and 120°, respectively; in Fig. 4 at an incident neutron energy $E_n = 11.5$ MeV for outgoing angles of 60° and 120°, respectively.

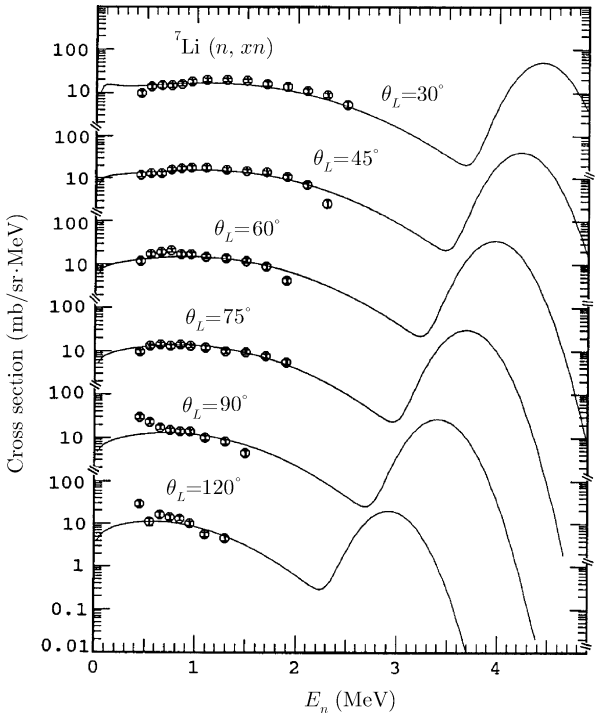

Fig. 1 The neutron energy-angular spectra of 30°, 45°, 60°, 75°, 90°, and 120° at E_n = 5.1 MeV. The data are taken from Ref. [4].

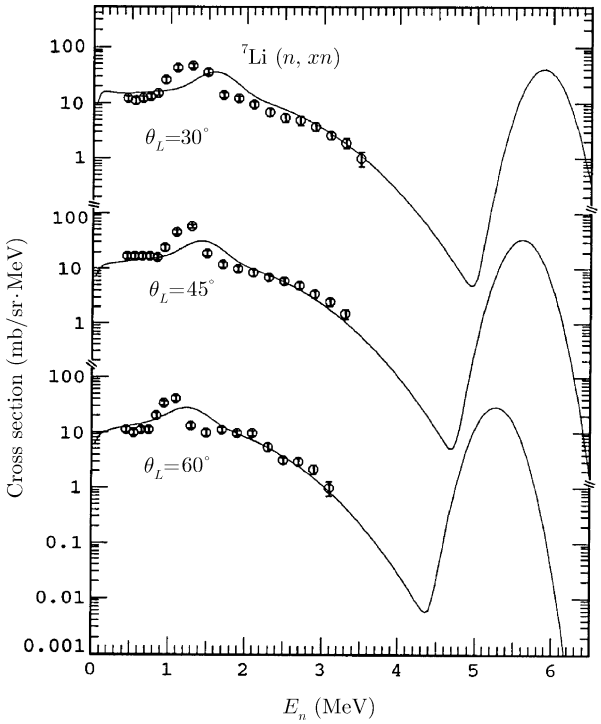

Fig. 2 The neutron energy-angular spectra of 30°, 45°, and 60° at E_n = 6.6 MeV. The data are taken from Ref. [4].

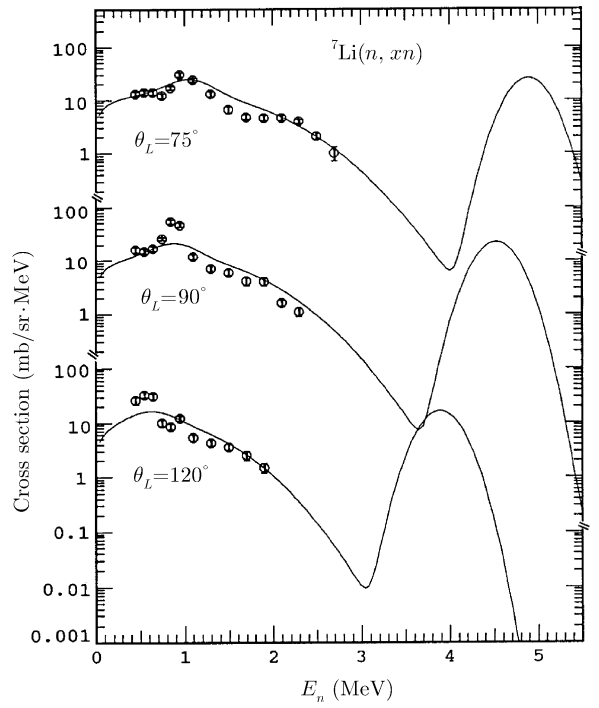

Fig. 3 The neutron energy-angular spectra of 75°, 90°, and 120° at E_n = 6.6 MeV. The data are taken from Ref. [4].

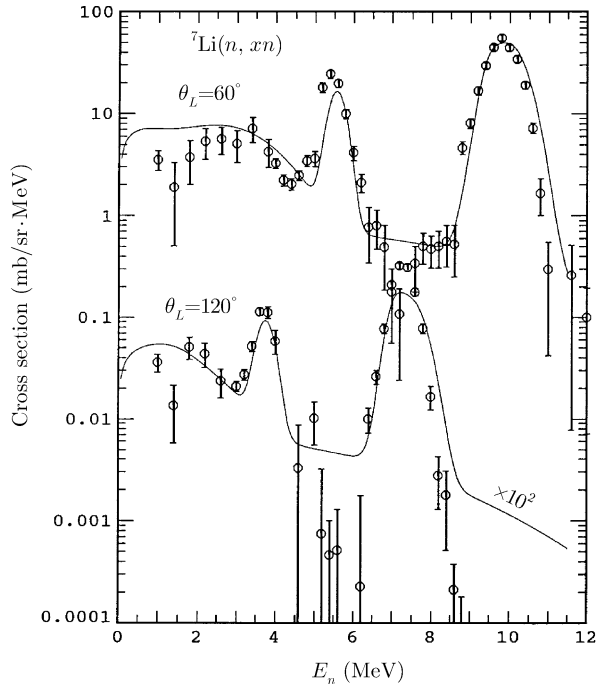

Fig. 4 The neutron energy-angular spectra of 60° and 120° at E_n = 11.5 MeV. The data are taken from Ref. [7].

Meanwhile, the comparisons of the outgoing neutrons at an incident neutron energy $E_n = 14.2$ MeV for outgoing angles of 30°, 37.5°, 43.12°, 50°, 60°, 75°, 94.28°, 104.2°, and 150° are shown in Figs 5 ~ 7, where the elastic scattering peak is not added, by which the inelastic scattering partial spectrum is overlapped. As an example, we show here in Fig. 8 the total neutron energy-angular spectrum at $E_n = 14.2$ MeV for the outgoing angle 60°, in which the added elastic scattering peak overlaps the inelastic scattering peak. This is the reason why many of the measurements for the elastic scattering cross sections are always together with the inelastic scattering cross section. The comparisons of the outgoing neutrons spectra at an incident neutron energy $E_n = 18$ MeV for the outgoing angles 20°, 30°, 37.5°, 45°, 52.5°, 60°, 70°, 80°, 90°, 105°, 120°, 135°, and 150° are shown in Figs 9 ~ 11. All of the fittings in this paper agree fairly well with the measurements.

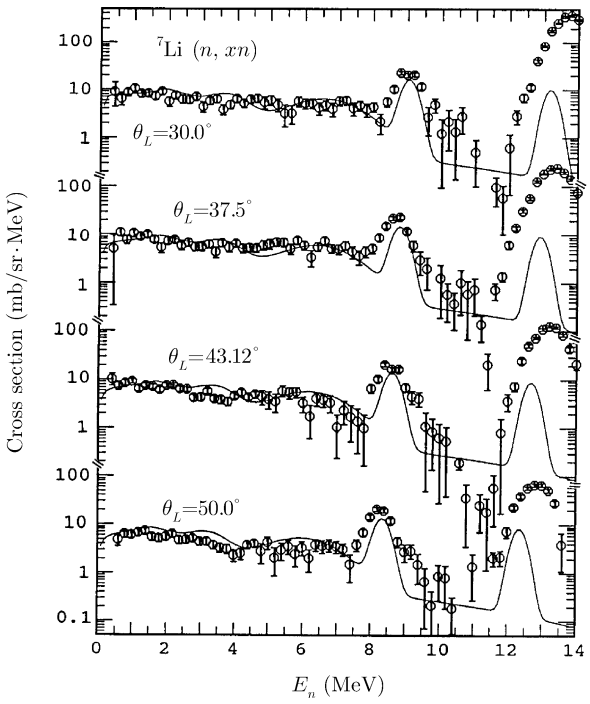

Fig. 5 The neutron energy-angular spectra of 30.0°, 37.5°, 43.12°, and 50.0° at $E_n = 14.2$ MeV. The data are taken from Ref. [5].

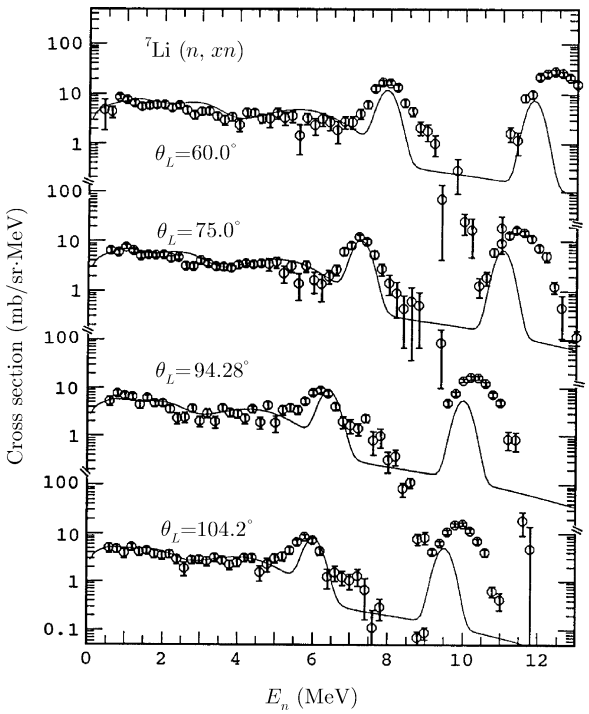

Fig. 6 The neutron energy-angular spectra of 60.0°, 75.0°, 94.28°, and 104.2° at $E_n = 14.2$ MeV. The data are taken from Ref. [5].

As an example, the calculated cross sections from discrete level to discrete level, the energies of the first emitted particles in CMS, and the energy region of the residual nucleus after the second particle emissions are shown in Table 3 at $E_n = 14.2$ MeV. The recoil effect of the secondary particle emissions is very strong in light nucleus reactions. In general the nucleon emissions (neutron or proton) give energy region with several hundred keV of the ring-type spectra, while the triton emissions give the large energy region with a few MeV, due to the relative heavier mass. However, all of the ring-type spectra must be treated as the continuum spectra to keep the energy balance. The third row in Table 3 corresponds to the energy region in the ring-type spectra after the second particle emissions to show this fact.

The total energy-angular spectrum for each angle consists of many partial spectra from different reaction channels. This reaction situation, for example, in $\theta = 60°$ at 11.5 MeV is shown in Fig. 12. The high-energy components of the energy-angular spectrum mainly come from the first neutron emissions. The neutron from the three-body breakup of ^{6}He* only contributes to the low-energy region with the designation k.

The pre-equilibrium mechanism dominates the reaction processes of $n + ^7$Li below the energy 20 MeV, and the calculations indicate that only the equilibrium mechanism could not give the reasonable results even at low neutron-incident energies. At $E_n = 14.2$ MeV, as an example, the pre-equilibrium state occupies the percentage of $P_{\text{pre-eq}} = 57.6\%$, while the equilibrium state only has $P_{\text{eq}} = 42.4\%$.

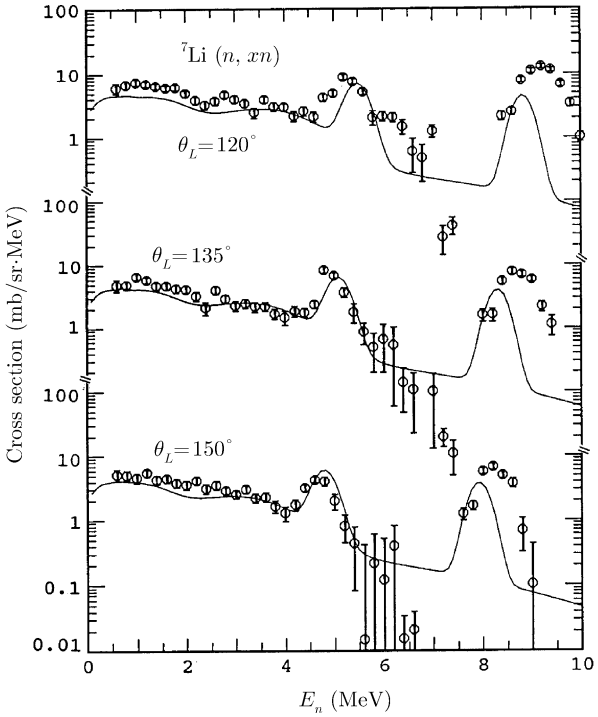

Fig. 7 The neutron energy-angular spectra of 120°, 135°, and 150° at E_n = 14.2 MeV. The data are taken from Ref. [5].

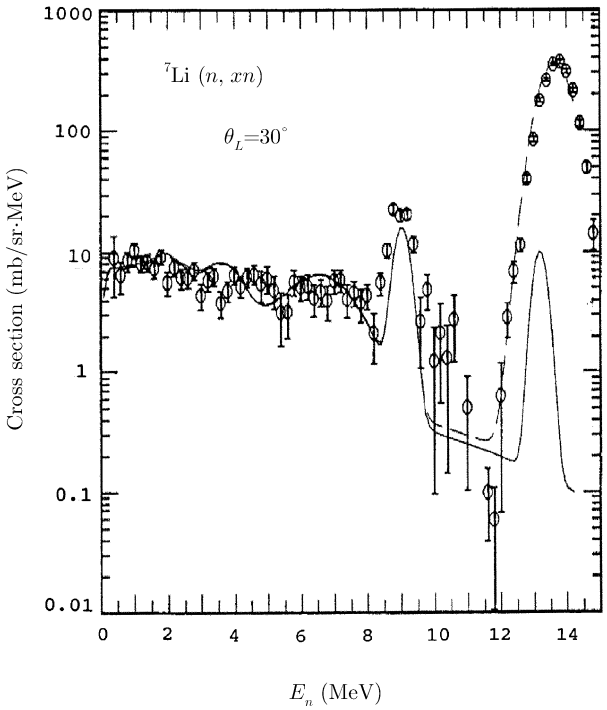

Fig. 8 The neutron energy-angular spectra of 30° at E_n = 14.2 MeV. The data are taken from Ref. [5]. The added elastic scattering peak is plotted by dashed line.

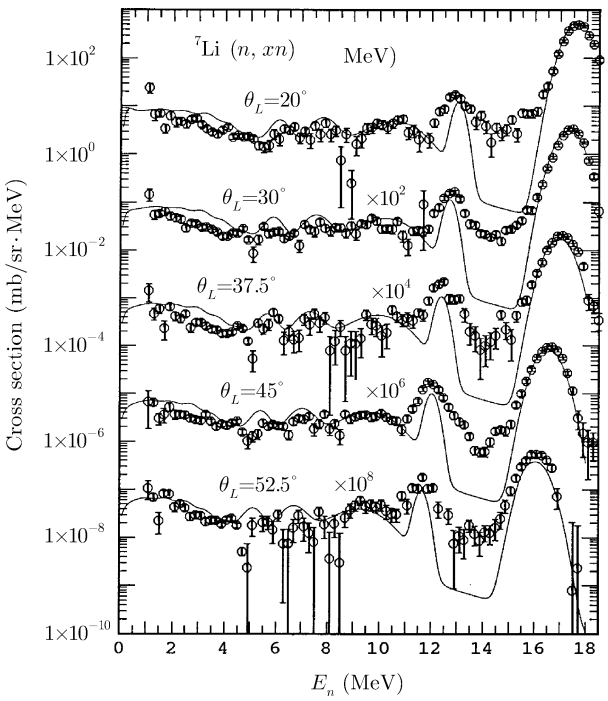

Fig. 9 The neutron energy-angular spectra of 20°, 30°, 37.5°, 45°, and 52.5° at E_n = 18 MeV. The data are taken from Ref. [7].

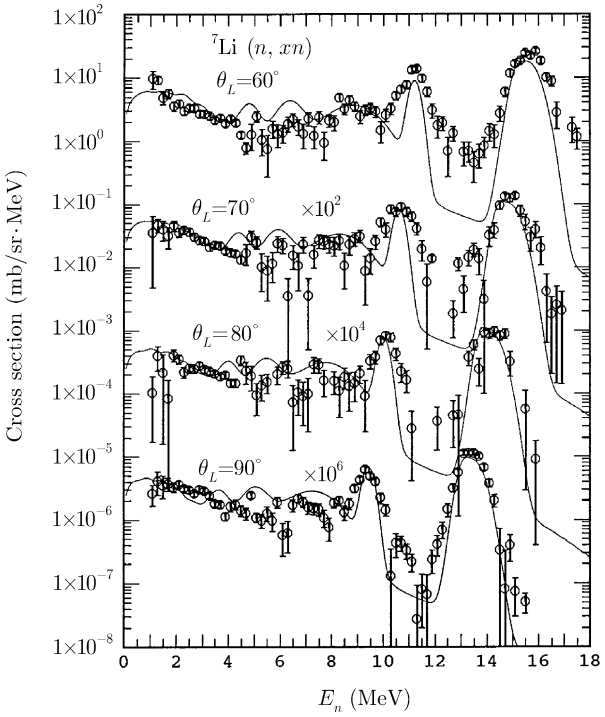

Fig. 10 The neutron energy-angular spectra of 60°, 70°, 80°, and 90° at E_n = 18 MeV. The data are taken from Ref. [7].

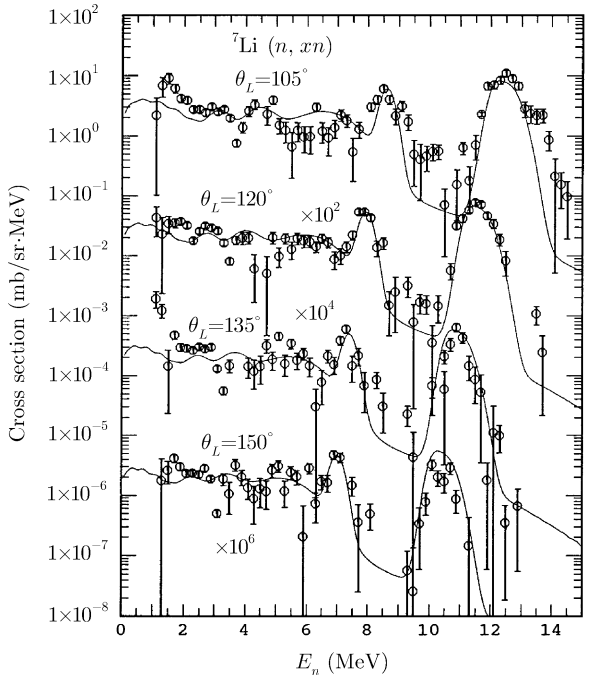

Fig. 11 The neutron energy-angular spectra of 105°, 120°, 135°, and 150° at E_n = 18 MeV. The data are taken from Ref. [7].

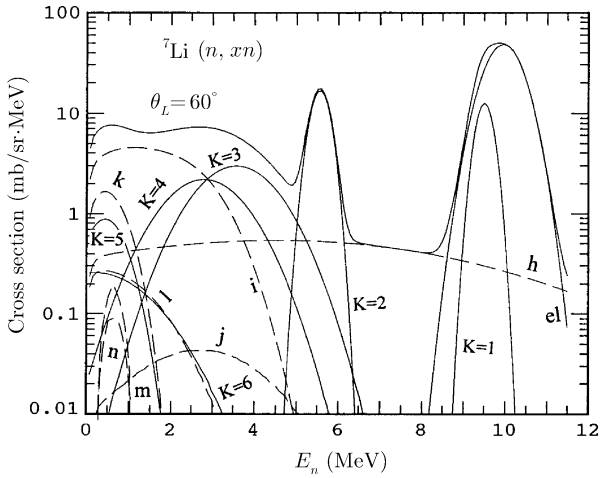

Fig. 12 The partial spectra of the secondary neutrons of 60° at E_n = 11.5 MeV. Designations K = 1 through K = 6 correspond to the first emitted neutron from the compound nucleus ^{8}Li* to the $K_{\rm th}$ excited levels of ^{7}Li*, respectively; designation el corresponds to the elastic scattering peak; designations i and h correspond to the emitted neutrons from ^{5}He as the residual nucleus of (n, t) channel, respectively, at the ground state and the first excited state; designation k corresponds to the neutrons from the three-body breakup process of ^{6}He* as the residual nucleus of the (n, d) channel; designations l and j correspond to the neutrons from the fourth and sixth excited levels of ^{7}Li to the ground state of ^{6}Li of the $(n, 2n)$ channel; designations m and n correspond to the neutrons from the fifth and the sixth excited levels of ^{7}Li to the first excited level of ^{6}Li of the $(n, 2n)$ channel. The above full line is the calculated total energy-angular spectrum.

Table 3 The calculated cross sections of the partial reaction channels to the k_2 level of the residual nucleus via the k_1 level.

Channel	k_1	k_2	CS (mb)	$E(k_1)$[a]	ER2(min–max)[b]
(n,n)	1		47.38	10.443	
(n,d)	gs		5.38	3.501	
(n,d)	1		16.9	2.153	
(n,t)	gs		84.33	5.663	
(n,t)	1		41.05	3.162	
$(n,2n)$	4	gs	3.85	4.337	0.307–0.812
$(n,2n)$	5	gs	0.02	2.404	0.002–1.277
$(n,2n)$	5	1	2.41	2.404	0.129–0.526
$(n,2n)$	6	gs	8.21	2.246	0.007–1.285
$(n,2n)$	6	1	2.15	2.246	0.079–0.589
$(n,2n)$	7	gs	2.27	1.031	0.160–1.232
$(n,2n)$	7	1	1.7	1.031	0.023–0.744
$(n,2n)$	7	2	0.54	1.031	0.012–0.363
(n,np)	7	gs	0.72	1.031	0.005–0.609
(n,nd)	6	gs	0.93	2.246	0.049–0.54
(n,nd)	7	gs	3.09	1.031	0.127–1.009
(n,nt)	2	gs	60.58	6.811	0.048–2.916
(n,nt)	3	gs	51.31	5.019	0.496–3.932
(n,nt)	4	gs	41.37	4.337	0.754–4.232
(n,nt)	5	gs	22.31	2.404	1.728–4.838
(n,nt)	6	gs	9.14	2.246	1.825–4.869
(n,nt)	7	gs	2.03	1.031	2.720–4.967
(n,pn)	gs	gs	16.33	1.747	0.044–0.511

[a] $E(k_1)$ refers to the emitted energy for the first emitted particle in CMS.

[b] ER2(min–max) refers to energy region in the ring-type spectra of the residual nucleus after the second particle emissions.

5 Summary

The reaction mechanism of neutron induced ^{7}Li is very complex, all of the four possible kinematics of (D to D), (C to D), as well as (D to C) and (C to C) are included in the description of the energy-angular spectra with the energy balance analytically. If the residual nucleus was treated as a static nucleus in CMS, then neither the reasonable shape of the energy-angular spectra nor the energy balance could be obtained in the model calculation.

The three-body breakup process is a special mechanism in the $n+^7$Li reactions. In this paper the description of the angular-energy spectra of the three-body breakup process following two particle emissions has been developed.

The level-broadening effect and energy resolution in measurements must be taken into account for fitting energy-angular spectra of outgoing neutrons. All of the level widths are taken from the experimental data as fixed parameters. So far there are no File-6 for double-differential cross sections of $n+^7$Li in the worldwide neutron data libraries, so only the isotropic spectra of the

outgoing particles are given in File-5, such as $(n, np)^6$He, $(n, 2nd)\alpha$, $(n, 3np)\alpha$, and $(n, 2n)^6$Li reaction channels, with the many-body phase space method. Meanwhile, only the neutron information of the reaction channel $(n, nt)\alpha$ was given by means of pseudo-levels as the inelastic scattering cross sections in File-3 without any information of outgoing charged particles. With this approach and based on the good fitting to the double-differential measurements the Files-6 of the reaction channels $(n, 2n)^6$Li, $(n, np)^6$He, $(n, 2nd)\alpha$, $(n, n\alpha)t$, and $(n, 3np)\alpha$ have been set up by using the LUNF code in the neutron data library with full energy balance. To do so in this way the pseudo-levels used in the present neutron libraries could be erased. The information of the energies released from the outgoing charged particles is needed in several applications. For example, the kerma factors are of specific interest regarding the heat produced in fusion reactors.

Acknowledgments

The authors would like to thank Dr. S. Chiba for providing their experimental data for analyses in the present work.

References

[1] J.S. Zhang, Y.L. Han, and L.G. Cao, Nucl. Sci. Eng. **133** (1999) 218.

[2] J.S. ZHANG and Y.L. HAN, Commun. Theor. Phys. (Beijing, China) **36** (2001) 437.

[3] J.S. ZHANG, Y.L. HAN, and X.L. FAN, Commun. Theor. Phys. (Beijing, China) **35** (2001) 579.

[4] M. Baba, *et al.*, Bull. American Phys. Soc. **24** (1979) 862.

[5] S. Chiba, *et al.*, J. Nucl. Sci. Tech. **22** (1985) 771.

[6] H, Xia, *et al.*, China J. Nucl. Phys. **15** (1993) 367.

[7] S. Chiba, private communication.

[8] J.S. Zhang, Nucl. Sci. Eng. **114** (1993) 55.

[9] R.B. Firestone and V.S. Shirley, *Table of Isotopes*, 8th edn., John Wiley & Sons (1996).

[10] G.G. Ohlson, Nucl. Instrum. Meth. **37** (1965) 240.